J. Cent. South Univ. Technol. (2008) 15(s2): 114−120
DOI: 10.1007/s11771−008−0445−5

Springer

Dynamic experimental study on rock meso-cracks growth by digital image processing technique

ZHU Zhen-de(朱珍德)[1, 2], NI Xiao-hui(倪骁慧)[1, 2], WANG Wei(王 伟)[1, 2],
LI Shuang-bei(李双蓓)[3], ZHAO Jie(赵 杰)[1, 2], WU Yi-quan(武沂泉)[1, 2]

(1. Geotechnical Research Institute, Hohai University, Nanjing 210098, China;
2. Key Laboratory of Ministry of Education for Geomechanics and Embankment Engineering, Hohai University, Nanjing 210098, China;
3. College of Civil Engineering and Architechure, Guangxi University, Nanning 530004, China)

Abstract: A new meso-mechanical testing scheme based on SEM was developed to carry out the experiment of microfracturing process of rocks. The microfracturing process of the pre-crack marble sample on surrounding rock in the immerged Long-big tunnel in Jinping Cascade II Hydropower Station under uniaxial compression was recorded by using the testing scheme. According to the stereology theory, the propagation and coalescent of cracks at meso-scale were quantitatively investigated with digital technology. Therefore, the basic geometric information of rock microcracks such as area, angle, length, width, perimeter, was obtained from binary images after segmentation. The failure mechanism of specimen under uniaxial compression with the quantitative information was studied from macro and microscopic point of view. The results show that the image of microfracturing process of the specimen can be observed and recorded digitally. During the damage of the specimen, the distribution of microcracks in the specimen is still subjected to exponential distribution with some microcracks concentrated in certain regions. Finally, the change law of the fractal dimension of the local element in marble sample under different external load conditions is obtained by means of the statistical calculation of the fractal dimension.

Key words: marble; rock failure process; digital image processing; growth of meso-crack; dynamic observation; experimental study

1 Introduction

The change of macromechanical behavior induced by the evolution of meso-structure of materials is a very important research subject of solid mechanics and material science. Rock is a multiphase material composed of several kinds of mineral grains, cements, micro-pores and cracks. The micro-pores and cracks have a random distribution of different ranks. The macroscopic fracture and failure of rock are closely related to the generation, distribution, propagation and coalescence of micro-cracks. MICHAEL et al[1] considered that the mechanism of micro-crack initiation could be investigated only after the establishment of multi-scale mechanics model. Brittle or ductile materials should be studied at the meso-level. Recently, the detection method for rock damage using SEM further impels the research on rock damage. In 1997, YOSSEF et al[2] studied the relationship between the micro-structure of dolomite, the initial stress of micro-crack initiation and ultimate strength of sample. They found that the micro-structure has a great impact on the ultimate strength. By conducting the compression experiment on Darley Dale sandstone, WU and BAUD[3] studied the evolution of anisotropic damage on micro-level with the optical microscope and SEM. They obtained the relationship between micro-crack density and strain. In 2000, PASCAL and MICHEL[4] analyzed the SEM images with digital speckle correlation techniques (DSCM). DWIVEDI et al[5] studied various themo- mechanical properties of Indian granite in the range of 30−160 ℃ by using SEM. In addition, a literature survey was carried out to collect data on the properties of granites at high temperatures. During 1992 to 1995 ZHAO et al[6−8] studied the growth of the damage on the marble plate with oblique cutting gap. LI et al[9] studied the growth of micro-crack on granite. The above researches play an important role in understanding the mechanism of rock damage. WANG et al[10] researched the microstructure and cell of rock by means of SEM. The fractal characteristics were analyzed by the dissipated energy consumed by the microstructure fracture. The form and direction of crack propagation in

Foundation item: Projects(50674040, 50539090) supported by the National Natural Science Foundation of China; Project(CX07B_128z) supported by the Cultivate Creative Postgraduate Foundation of Jiangsu Province, China
Received date: 2008−09−05; **Accepted date**: 2008−10−18
Corresponding author: ZHU Zhen-de, Professor, PhD; Tel: +86−13851886169; E-mail: zzdnj@hhu.edu.cn

rock were obtained according to the given loading by using fractal geometry method and micro-thought method. Using the high temperature fatigue testing system with scanning electron microscope, ZHAO et al[11] observed the influence of temperature's change on limestone's microstructure in real time. XIE et al[12] discussed the thermal damage evolution process, thermal crack growth and fracture characteristic of rock.

Nevertheless, there are few researches on the combination of the digital quantitative observation with direct observation. With the development of digital image processing, the combination becomes possible. Therefore, in this work, a new meso-mechanical testing scheme of whole process tracking quantitative observation was developed to carry out the experiment on microfracturing process of rocks. The digital quantitative analysis of Jinping marble in Sichuan Province under uniaxial compression was performed by means of scanning electron microscopy (SEM). This combination method founded the testing basis for the theoretical analysis and numerical calculation of the meso-damage mechanism of rock.

2 Meso-mechanical test on microcracks growth of tracing rock

Meso-mechanical test scheme on tracing rock microcracks growth can make it possible for the observation displaying all rock failure process in uniaxial compression test. By servo control on load and deformation, loading and data acquisition on rock samples can be realized synchronously and effectively.

2.1 Rock sample and test device

The rock samples were marbles collected in the site of Sichuan Jinping Hydropower Station (Jinping Hydropower Station is located in the main stream of Yaqing river in Liangshan, Sichuan, China). In order to ensure the uniformity of samples, the samples were collected from the same bloc. The selected marble samples were mainly white, locally a little black, composed of carbonate mineral components, and mainly had a fine granular crystalloblastic texture, partly a coarse granular crystalloblastic texture, and a good macroscopic homogeneity. For the convenience of test observation and image collecting, the samples were processed by surface polishing and gold plating after cutting and slotting (the processing flow is shown in Fig.1 and the samples are shown in Fig.2), and the samples were marked in proper location at the same time.

The test device system (Fig.3) mainly includes: HITACHI S-570 SEM (the resolution is 3.5 nm; the highest accelerated voltage is 30 kV; the magnification is greater than 50 000 times) and the new servo loading system (the load ranges from 0 to 2 000 N; the measurement error is $\pm$0.5 N; the stroke of tension and compression is from 0 to 10 mm; the measurement error in displacement is 1 μm) developed by the Mechanical Institute.

2.2 Image collecting on meso-structure of rock micro-cracks growth

In the loading processing, SEM was used to observe and record the development and collection of each microcrack on the surface of samples under different horizontal loading conditions. When referring to the digital image collecting, there are mainly the following two problems to be taken into account.

1) The magnification of image determines the scale and effect of observation for microcracks because of the mutual restriction between the magnification and display range of the image. In order to get a good effect of micro-scale observation, taking into account Refs.[11−12] and specific conditions in this test, the magnifications adopted are 50, 100 , 300 times, respectively. Meanwhile, considering the effect of observation, the magnifications in local area are 500, 1 000 times, respectively.

2) Once the magnification is established, the accuracy of statistics information such as the quantity of microcracks is determined by the quantity of image collecting and sequence. In order to obtain more comprehensive information, this test adopted layering from the upper to under, collecting from the left to the right by using the signs marked on samples in advance so as to obtain the maximum information and avoid obtaining image information repeatedly.

2.3 Rock meso-structure SEM images processing program

In recent years, with the development of computer technology and digital image processing technology, it

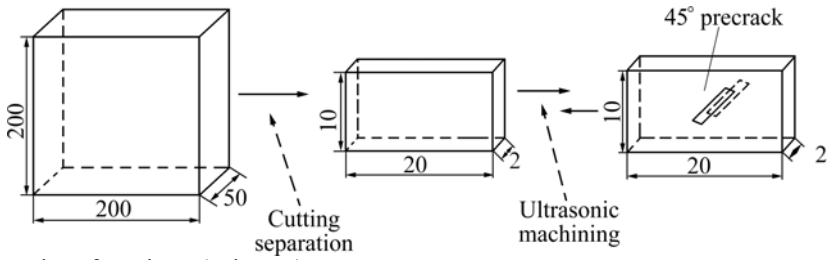

Fig.1 Flowchart of preparation of specimen (unit: mm)

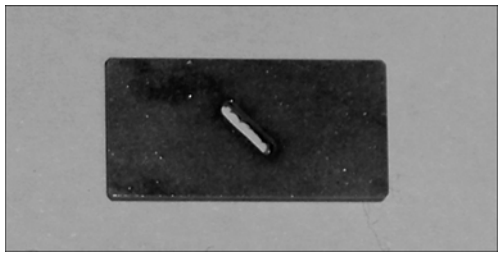

Fig.2 Specimen 1

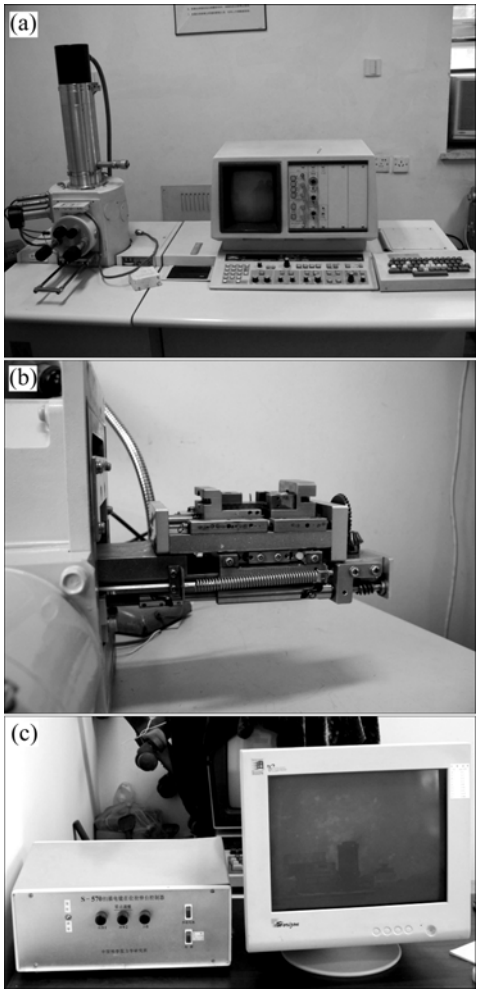

Fig.3 Test device system about meso-mechanical testing scheme based on SEM: (a) HITACHI S-570 SEM**;** (b) Loading device**;** (c) Servo control system

becomes feasible that the characteristic information of rock meso-structure is quantified with the analysis of meso-image of rock samples[13−14]. With the development of digital image processing technology, it is easier, more accurate, more representative in statistics to obtain data from meso-image of samples. The datamation of image of rock microcracks by SEM belongs to the module of image analysis treatment in digital image processing. Based on the characteristics of rock meso-structure SEM images, the region growing method was used for image segmentation, and the relative image recognition program was compiled by combining image processing toolbox in Matlab[14], so SEM image data were obtained accurately (Fig.4).

3 Test results and analysis

3.1 Fracture process of microcrack

To show the validity and correctness of the test, the initiation, growth and coalescence of a microcrack on sample 1 were analyzed (see Figs.5 and 6). In the analysis, all the 'cracks' mentioned mean cracks developed in the test. For precrack, it is designated especially.

3.2 Statistics and analysis of test data

3.2.1 Statistics of data

Using the self-programmed SEM images processing software for rock meso-structure[13−14], the SEM micro-crack images of sample 1 on stages of initiation, growth and coalescence were analyzed and the geometric data of microcracks in the entire fracture process were as follows: area, length, azimuth, width, perimeter of microcrack corresponding to different stress states (as there are too many data , only a part were cited in Table 1).

After statistical analysis based on the geometry data, the total area of the microcrack (Fig.7) and the relationships between stress and area, width, length and azimuth were obtained in Table 2.

3.2.2 Mechanism analysis of microcrack growth under uniaxial compression loading

In the preliminary stage of loading, part OA of the stress—strain curves (Fig.8) and the total area of microcrack (for $\bar{\sigma}$=20 MPa and $\bar{\sigma}$=30 MPa in Fig.7) show that the mirocracks between the marble grains are compressed. Moreover, the bearing surface of grain increases gradually under loading, and from the point of macroscopic view, the rigidity increases too. In this stage, the total area of microcrack changes little and the compression microcracks dominated. As the load increases, the slope of the curve between A and B becomes sharper. This shows that the local nonlinear deformation increases the rigidity. At the macro scale, the sample is in elastic stage. At the meso scale, because of different geometric and physical properties of marble grains and stress concentration, microcracks dispersively distribute and a few of them gather together in the process (Fig.6(d)). With increasing load, under the stress and strain condition decided by micro-fracture, the former dispersively distributed microcracks grows approximately perpendicular to the direction of precrack in opening mode. At the same time, new dispersively distributed microcracks appear because of inhomogeneous distribution of stress around the microcracks. In consequence, some microcracks gathered together and two wider cracks appear (Fig.6(e)). The total area of microcracks increases rapidly (Fig.7). When

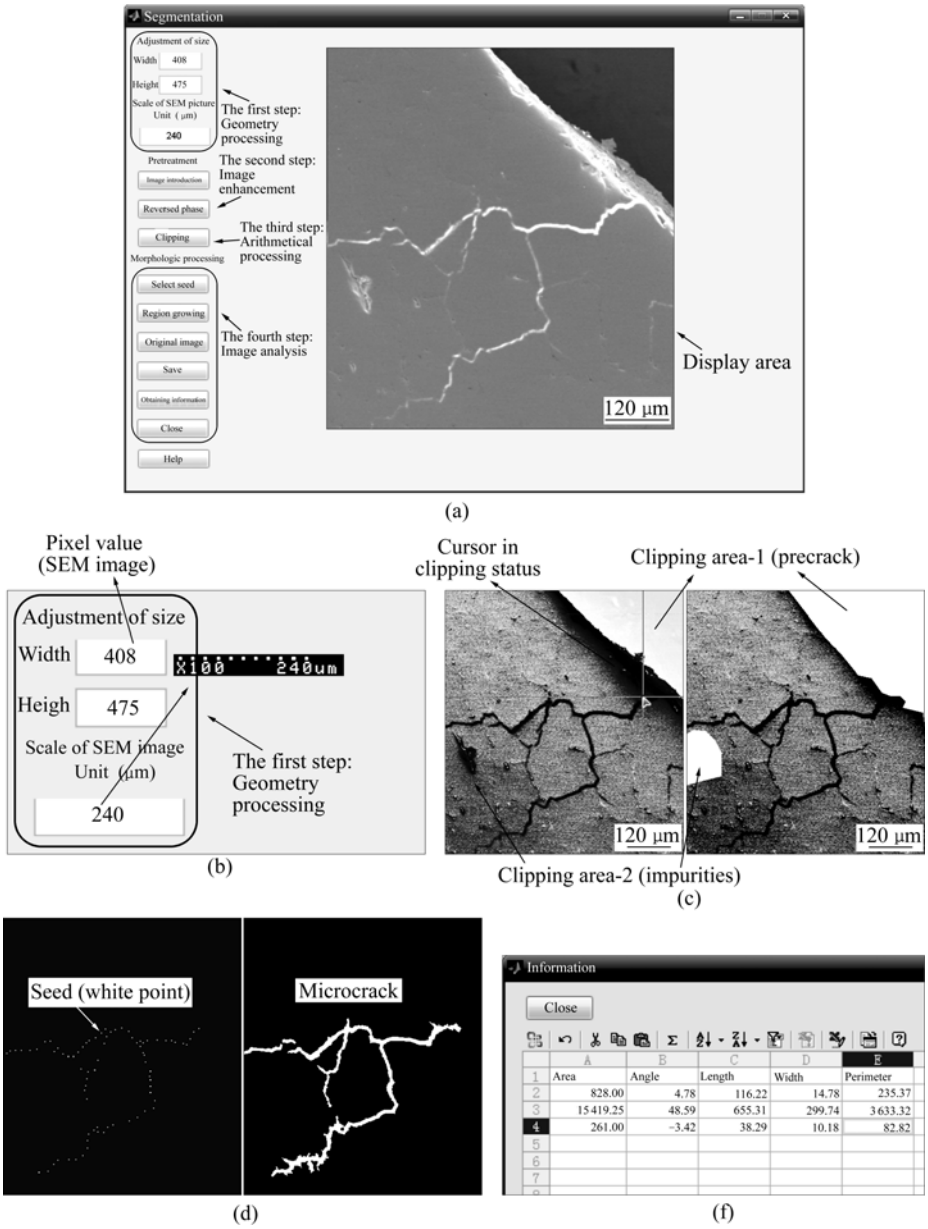

Fig.4 Introduction of program for datamation of image: (a) Operation of image processing program; (b) Adjustment of size; (c) Clipping algorithm; (d) Image segmentation of regional growing; (e) Statistical data of image

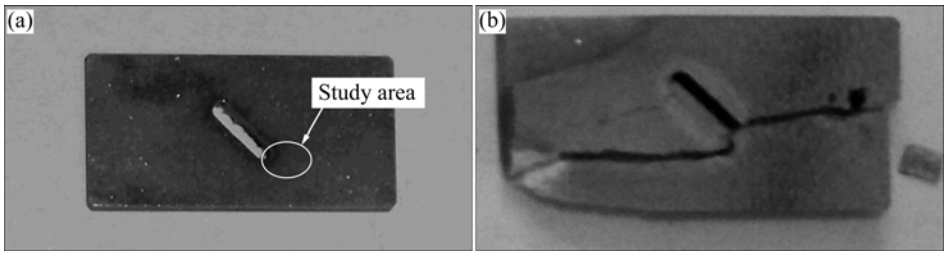

Fig.5 Photos of specimen 1: (a) Pre-test; (b) After test

the load increases to a higher level, the azimuth of new microcrack changes from the direction approximately perpendicular to the precrack to the loading direction. Crack 2 which predominates in the direction grows faster than crack 1 whatever in length, area, and width (Table 2). The curve between *B* and *D* corresponding to the failure stage is very short. The SEM image of rock sample in the state of ultimate stress (point *C*) is very difficult to capture. At the meso scale, the main crack grows rapidly approximately in the loading direction. The effective bearing area of the sample decreases sharply and stress highly concentrates in the microcrack

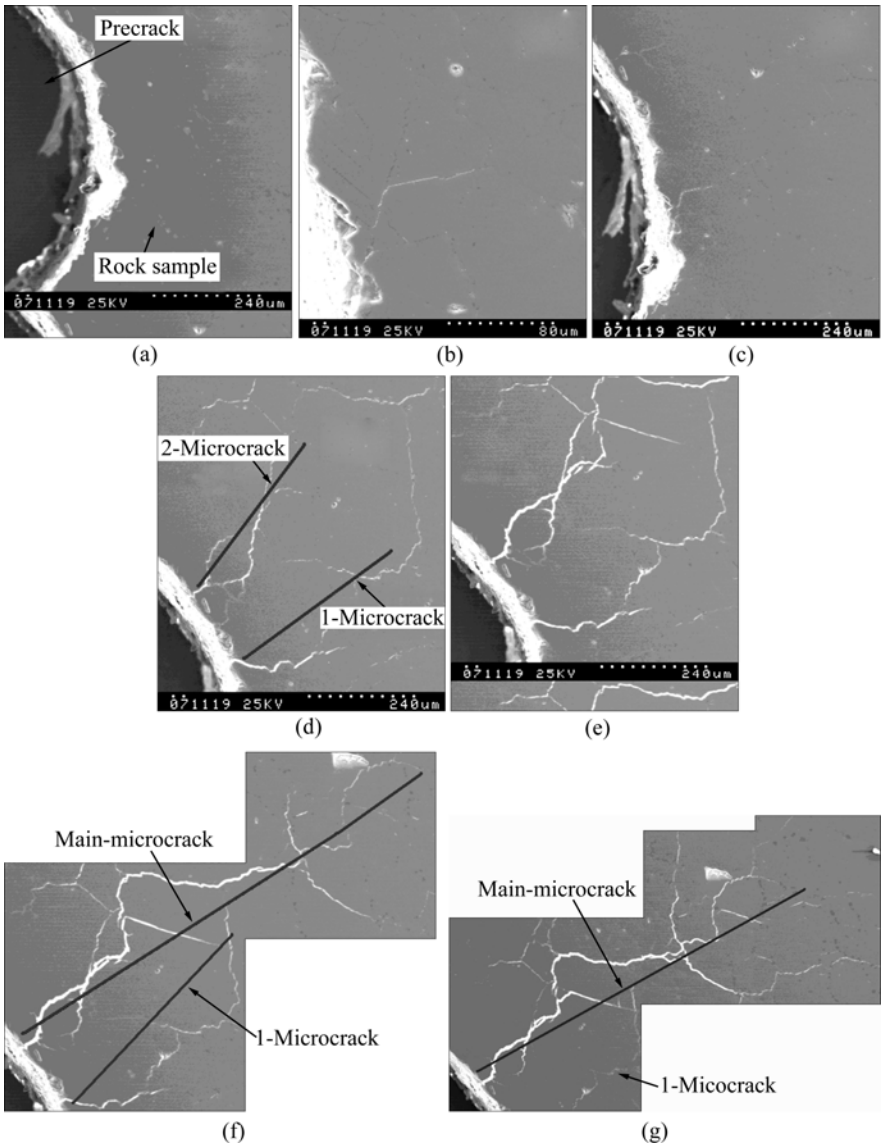

Fig.6 SEM images showing process of surficial microcrack development and macrofracture formation in specimen 1 under different uniaxial compressions: (a) 0 MPa; (b) 20 MPa; (c) 30 MPa; (d) 45 MPa; (e) 50 MPa; (f) 55 MPa; (g) 60 MPa

Table 1 Partial geometric data of microfracture about specimen 1 ($\bar{\sigma}$ =0 MPa)

Number	Area/ μm^2	Azimuth/ (°)	Length/ μm	Width/ μm	Perimeter/ μm
1−1	13.50	65.54	12.41	2.04	25.31
1−2	194.25	15.02	92.04	11.69	193.83

dense region. At this time, the sample is in a precarious balance and minor disturbance will cause brittle failure. The cracks continue to grow when the stress is kept at 60 MPa. This means that the energy consumed by grain deformation and growth of crack cannot balance the release of the accumulated energy. When the stress reaches 61 MPa (Fig.8), the main crack interpenetrates rapidly in a direction parallel to loading axis. Axial splitting occurs and there is a shear failure plane throughout the sample (Fig.5(b)).

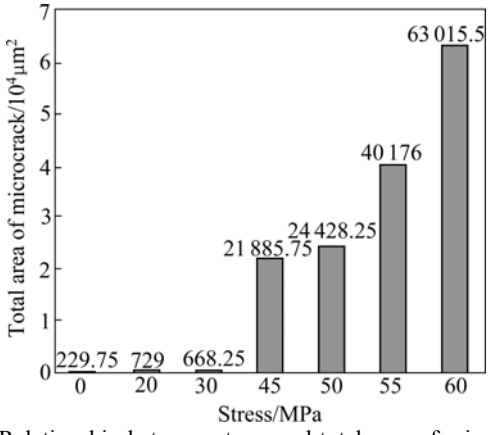

Fig.7 Relationship between stress and total area of microcrack of specimen 1

3.2.3 Statistical analysis of microcrack spacing in failure process

Spacing is one of the important parameters that

Table 2 Relationships between stress and area, average width, length, azimuth in loading process

Stress/ MPa	Crack 1				Crack 2			
	Area/ μm^2	Average width/ μm	Length/ μm	Azimuth/ (°)	Area/ μm^2	Average width/ μm	Length/ μm	Azimuth/ (°)
45	5 247.00	17.03	244.26	46.14	5 206.50	12.54	223.59	73.08
50	9 672.75	21.68	478.54	49.79	10 104.75	27.57	503.72	59.16
55	3 474.00	13.51	456.24	51.03	30 629.25	29.64	1 052.19	37.66
60	Approximately closed				44 408.25	39.82	1 811.48	10.69

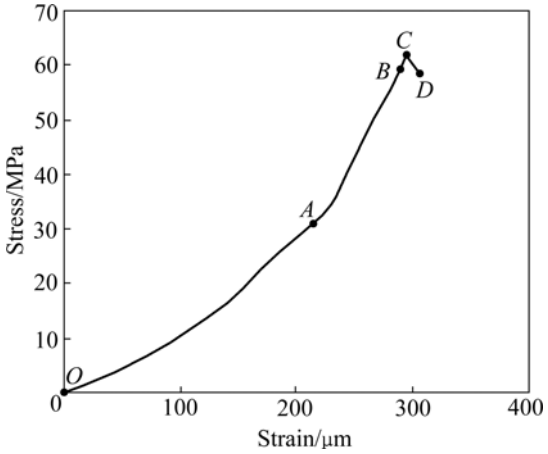

Fig.8 Stress—strain curve of specimen 1

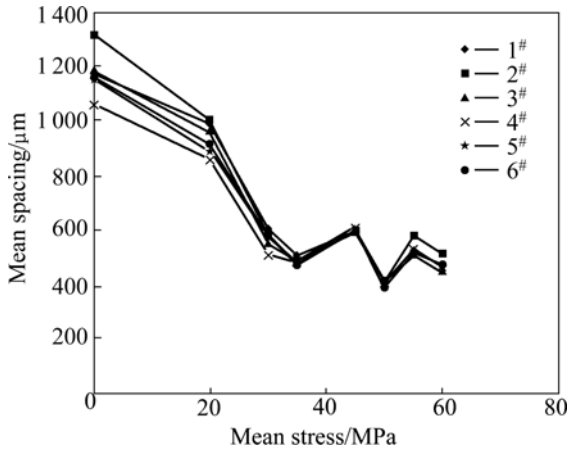

Fig.9 Statistical graph of average space of microcracks in all specimen under uniaxial compression

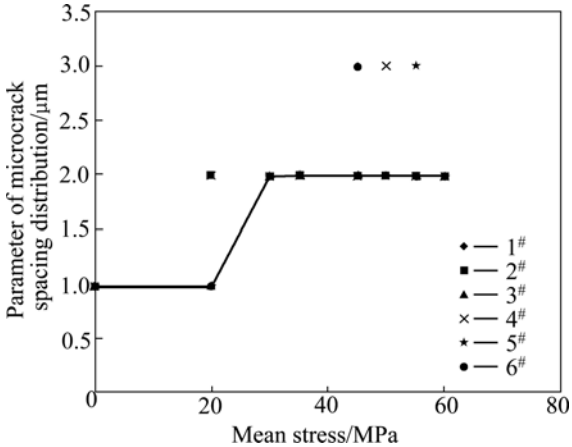

Fig.10 Graph of distribution parameter of average space of microcrack

characterize the microcrack. It directly reflects the distribution of microcracks and characterizes the damage degree and permeability of rock. In this work, as in Ref.[14], the following formula was used:

$$\lambda = \frac{L}{N_{LC}} \tag{1}$$

where L represents the length of dissect line along a particular direction and N_{LC} denotes the number of micro-crack crossed by the dissect line.

The statistical analysis of microcrack spacing in the whole process on samples 1 to 6 was performed (Fig.9). One of the nonparametric tests called K-S test was conducted for the statistical analysis of the microcrack spacing. It is found that microcrack spacing obeys the exponential distribution. The density function is:

$$f(s)=\lambda\exp(-\lambda s),\ s\geqslant 0 \tag{2}$$

where λ is a positive constant. The parameters of microcrack spacing distribution were calculated with the point estimation method (see Fig.10).

In Fig.10, five points lie out of the polygonal line and two of them coincide at point (20, 0.002). There are 37 points in the polygonal line, so the line can be regarded as the change process of average spacing distribution parameter. In the failure process, when $\bar{\sigma} \leqslant$ 30 MPa, compaction of microcrack dominates and the average spacing distribution parameter is 0.001. From $\bar{\sigma}$ =30 MPa to failure, all kinds of damage of microcracks dominate. The average spacing distribution parameter is 0.002 and remains unchanged. Therefore, the distribution of microcracks is relatively homogeneous and the distribution obeying certain exponential form is unchanged until the failure of the specimen.

3.2.4 Statistical analysis of element fractal dimension in failure process

With fractal geometry, irregular, disorderly phenomena in nature can be quantitatively described. Using box counting dimension method, the element fractal dimension was calculated[15].

The box counting dimension D_f is calculated as follows:

$$D_f = -\lim_{r\to\infty}\frac{\ln N(r)}{\ln r} \quad (3)$$

where r represents the side length of grid and $N(r)$ denotes the number of micro-cracks that cross the grids.

When $\bar{\sigma} \leqslant 20$ MPa (Fig.11), the fractal dimension of microcracks in compacting stage changes little. When $\bar{\sigma} \geqslant 20$ MPa, the fractal dimension of microcracks in damage development stage presents a linear variation. With the increase of average stress, the fractal dimension increases linearly until micro-transfixion occurs. The statistics of fractal dimension of six marble pre-crack samples show that fractal dimension is 1.59±0.05.

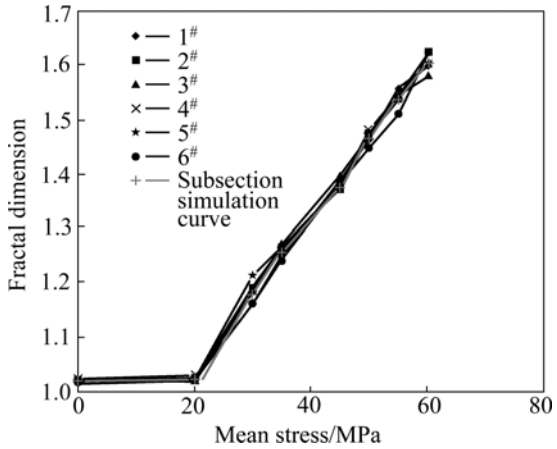

Fig.11 Statistical graph of relation average stress-fractal dimension

4 Conclusions

1) Meso-mechanical test scheme on tracing rock microcrack growth is designed in order to obtain the quantitative meso-mechanical information in rock failure process.

2) A SEM images processing program for rock meso-structure is compiled to process rock microcracks SEM image. Thus, the parameters such as the microcrack length, azimuth angle, width, area and perimeter, etc. can be extracted from microcrack structure under different stress states.

3) Combining stress—strain graph, SEM image and statistical data in the corresponding process, the microscopic mechanism of the microcrack growth and the effects on macroscopic property of samples in failure process of samples under uniaxial compression can described.

4) Based on statistical analysis, it can be seen that although microcracks are centralized in some areas, the distribution form, which obeys certain exponential function until the final failure of sample, keeps invariant.

5) Through statistical analysis on local frame element fractal dimension, it can be concluded that fractal dimension of marble at the stage of meso-damage basically presents linear trend as stress increases and when microcracks become transfixed and form macro cracks, the fractal dimension is 1.59 ± 0.05.

Acknowledgement

The help and support of professor LI Duan-yi at LMN laboratory in Mechanical Institute of Chinese Academy of Sciences are gratefully acknowledged.

References

[1] MICHAEL E K, SIA N N, SUO Z G. New directions in mechanics [J]. Mechanics of Materials, 2005, 37: 231−259.

[2] YOSSEF H H, ALON Z, YAAKOV M. Microstructure effects on microcracking and brittle failure of dolomites [J]. Tectonophysics, 1997, 281: 141−161.

[3] WU X Y, BAUD P W. Micromechanics of compressive failure and spatial evolution of anisotropic damage in Darley Dale sandstone Teng-fong [J]. International Journal of Rock Mechanics and Mining Sciences, 2000, 37(1): 143−160.

[4] PASCAL D, MICHEL B. Micromechanical application of digital speckle correlation techniques [M]. Springer-Verlag, 2000: 67−74.

[5] DWIVEDI R D, GOEL R K, PRASAD V V R, AMALENDU SINHA A S. Thermo-mechanical properties of Indian and other granites [J]. International Journal of Rock Mechanics and Mining Sciences, 2008, 45(3): 303−315.

[6] ZHAO Yong-hong, HUANG Jie-fan, WANG Ren. Real time observation of microfracturing process in rock during compression test [J]. Chinese Journal of Rock Mechanics and Engineering, l992, 11(3): 284−294. (in Chinese)

[7] ZHAO Yong-hong, HUANG Jie-fan, WANG Ren. SEM study of fracture development in compressed marble specimen and implications for earthquake precursors [J]. Chinese Journal of Geophysics, l993, 6(4): 453−462. (in Chinese)

[8] ZHAO Yong-hong, HUANG Jie-fan, HOU Jian-jun. Experimental study of meso-fractures in rock and its implication for understating seismic activities [J]. Chinese Journal of Geophysics, 1995, 38(5): 627−635. (in Chinese)

[9] LI L, TSUI Y, LEE P K K. Progressive cracking of granite plate under uniaxial compression [J]. Chinese Journal of Rock Mechanics and Engineering, 2001, 21(7): 940−947. (in Chinese)

[10] WANG Ze-yun, LIU Li, LIU Bao-xian. Characteristics of damage evolution of micropore and microcrack in rock [J]. Chinese Journal of Rock Mechanics and Engineering, 2004, 23(10): 1599−1603. (in Chinese)

[11] ZHAO Peng, XIE Wei-hong, WANG Xi-shu, CAO Feng. The real time experimental research on rock's SEM under high temperature [J]. Mechanics in Engineering, 2006, 28(3): 64−67. (in Chinese)

[12] XIE Wei-hong, GAO Feng, LI Shun-cai, GUAN Xiang-hui. Study on mechanism of thermal damage fracture for limestone [J]. Rock and Soil Mechanics, 2007, 28(5): 1021−1025. (in Chinese)

[13] ZHU Zhen-de, QU Wen-ping, JIANG Zhi-jian. Quantitative test study on mesostructure of rock [J]. Chinese Journal of Rock Mechanics and Engineering, 2007, 26(7): 1313−1324. (in Chinese)

[14] QU Wen-ping. Quantitative mesostructure investigation of rock based on digital image processing technique [D]. Nanjing: Hohai University, 2006. (in Chinese)

[15] LI Dao-wei. Mesomechanics experimental research on surrounding rock in immerged long-big tunnel [D]. Nanjing: Hohai University, 2008. (in Chinese)

(Edited CHEN Wei-ping)